Structural analysis of anodic porous alumina used for resistive random access memory

2010 Sci. Technol. Adv. Mater. 11 025002

(http://iopscience.iop.org/1468-6996/11/2/025002)

IOP PUBLISHING SCIENCE AND TECHNOLOGY OF ADVANCED MATERIALS

Sci. Technol. Adv. Mater. **11** (2010) 025002 (4pp) doi:10.1088/1468-6996/11/2/025002

Structural analysis of anodic porous alumina used for resistive random access memory

Jeungwoo Lee[1], Seisuke Nigo[1], Yoshihiro Nakano[2], Seiichi Kato[1], Hideaki Kitazawa[1] and Giyuu Kido[1]

[1] National Institute for Materials Science, 1-2-1, Sengen, Tsukuba, Ibaraki 305-0047, Japan
[2] GIT Japan Inc., 2-3-3, Shin-Yokohama, Kohoku-Ku, Yokohama 222-0033, Japan

E-mail: LEE.Jeungwoo@nims.go.jp

Received 16 November 2009
Accepted for publication 3 February 2010
Published 20 April 2010
Online at stacks.iop.org/STAM/11/025002

Abstract
Anodic porous alumina with duplex layers exhibits a voltage-induced switching effect and is a promising candidate for resistive random access memory. The nanostructural analysis of porous alumina is important for understanding the switching effect. We investigated the difference between the two layers of an anodic porous alumina film using transmission electron microscopy and electron energy-loss spectroscopy. Diffraction patterns showed that both layers are amorphous, and the electron energy-loss spectroscopy indicated that the inner layer contains less oxygen than the outer layer. We speculate that the conduction paths are mostly located in the oxygen-depleted area.

Keywords: porous alumina, nanostructure, ReRAM

1. Introduction

Anodic porous alumina (APA) has been used in various fields, for example, in the fabrication of nanomaterials and masks for photonic, electronic and optoelectronic systems, which utilize its highly ordered porous structure [1]. APA consists of two layers: an outer layer adjacent to the hole and an inner layer away from the hole [2]. A schematic diagram of porous alumina is shown in figure 1. The specific microstructure of APA results in unusual electrical properties. For example, Hickmott reported negative resistivity in anodic alumina [3], and the present authors revealed a bistable switching property and memory effect in APA that can be applied in resistive random access memory (ReRAM) [4]. The operation of ReRAM is based on a change in resistance induced by an applied voltage. Recently, ReRAM has attracted much attention because of the possibility of realizing a next-generation universal memory with high-speed, high-density and nonvolatile properties [5, 6]. ReRAM consists of a simple capacitor, in which an insulator (transition-metal oxide) is sandwiched between metal electrodes. Our investigation of ReRAM devices without the transition-metal led to the discovery of APA-based ReRAM. In this paper, we investigated the nanostructure of APA and its switching property, with the aim of its application of ReRAM.

2. Experimental details

2.1. Fabrication of anodic porous alumina

We fabricated the APA thin film for a ReRAM memory cell using a two-step anodization process with the aim of producing highly ordered nanosized holes [7]. The surface of an Al sheet (99.99%, 0.5 mm thickness) was electrochemically polished in a solution of perchloric acid and ethanol. The Al sheet was anodized at a constant voltage of 40 V in 0.3 M oxalic acid solution at 20 °C for 3 h. A platinum plate was used as a cathode. The distance between the cathode and the aluminum anode was 5 cm. Then the anodic oxide layer was removed by immersion in a mixture of phosphoric acid (6 wt%) and chromium oxide (1.8 wt%) at 60 °C for 1 h. Subsequently, the Al sheet was anodized again for 1 min under the same conditions as those in the first step. Finally, an upper

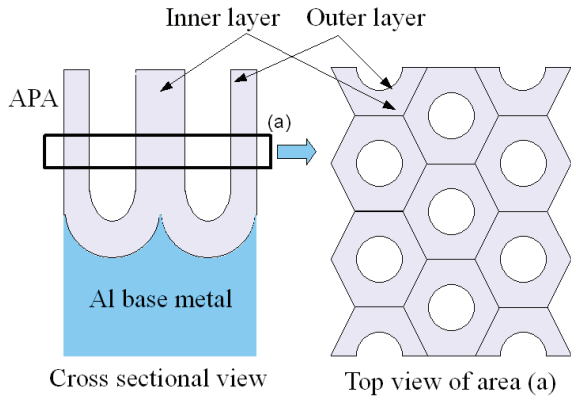

Figure 1. Cross-sectional and top-view schematic diagrams of fabricated porous alumina.

electrode with an 80 nm thick aluminum layer was deposited by thermal evaporation.

2.2. Characterization

The surface and cross-section morphologies of the APA thin film were observed using a field-emission scanning electron microscope (FESEM, JSM-6500F) and a high-resolution transmission electron microscope (HRTEM, H9500). The electronic structure of the film was studied by electron energy-loss spectroscopy (EELS, GIF/Model 863 Tridiem). Specimens with a thickness of less than 100 nm were prepared by focused ion beam (FIB) milling (FB-2100) after mounting them on a Cu mesh. A carbon coating was applied to protect the surface layer from the ion beam prior to FIB milling. The current–voltage (I–V) characteristics of the memory cell were measured using a Keithley 2400 sourcemeter unit at room temperature. We used a current-regulated diode (CRD) to prevent excessive current flowing through the memory cell in the set process. We also fabricated a micro size pattern on a SiO_2/Si substrate by conventional photolithography combined with an anodization process.

3. Results and discussion

3.1. Microstructure of anodic porous alumina

Figure 2(a) shows the APA surface topography observed using a SEM. The fabricated porous alumina has a pore diameter of 40 nm and an interpore distance of 100 nm with a 180 nm wall thickness. The corresponding bright-field TEM image is shown in figure 2(b). Part of the APA corresponding to the rectangular area in figure 1(a), was cut by FIB milling for the TEM observation. The selected-area diffraction patterns (beam spot size of 3–4 nm) of regions A (outer layer) and B (inner layer) reveal an amorphous structure for both layers. To clarify the difference between the two APA layers, we analyzed their electronic structures by EELS. A cross-sectional TEM image of APA is shown in figure 3, where 1 to 7 indicate the locations of the EELS measurements (spot size 1 nm, integration time 0.72 s point^{-1}). Point 1 is in the outer layer, point 2 is in the transition area from

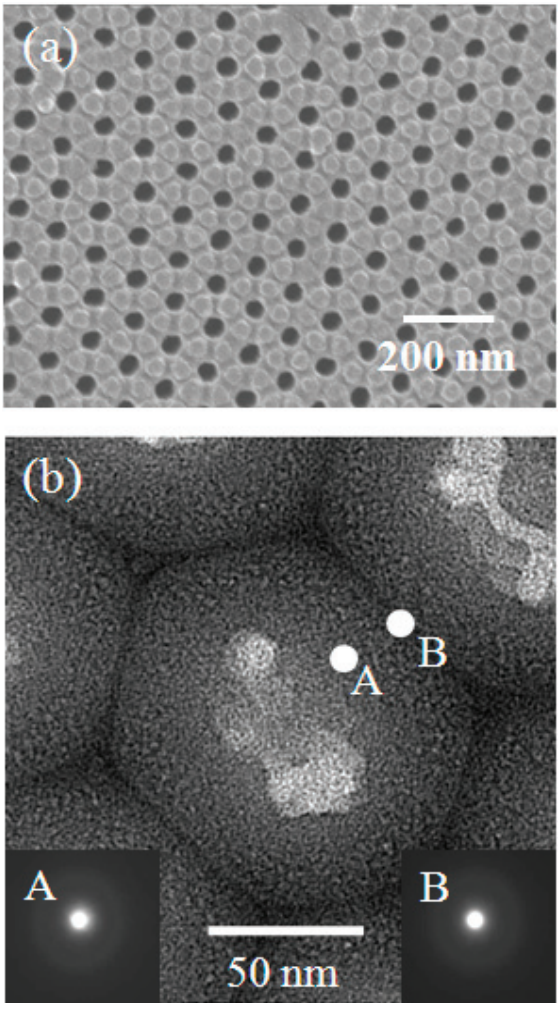

Figure 2. SEM (a) and bright-field TEM (b) images of APA produced using 0.3 M oxalic acid at 40 V. The insets of (b) show selected-area diffraction patterns at regions A (outer layer) and B (inner layer).

the outer layer to the inner layer, points 3 to 6 are in the inner layer and point 7 lies in the Al base metal. There is no significant variation between the Al L-edge spectra (not shown) for the outer and inner layers; on the other hand, the oxygen K-edge spectra exhibit a significant difference. A low-energy shoulder at 534 eV can be seen in the inner-layer spectrum (indicated by an arrow). This result suggests that the electronic states of oxygen in the inner layer are different from those in the outer layer. Jollet *et al* reported a similar shoulder at the O K-edge in Y_2O_3 [8]. The shoulder was stronger in their nonstoichiometric sample and was attributed to an oxygen vacancy. Iijima *et al* suggested from nuclear magnetic resonance analysis that porous alumina includes four- (AlO_4), five- (AlO_5) and six- (AlO_6) oxygen-coordinated aluminum atoms; the outer layer of porous alumina is composed of AlO_6, AlO_5 and AlO_4, and the inner layer is mostly AlO_5 and AlO_4 [9]. The outer layer oxidizes more easily than the inner layer, because it is in contact with the electrolyte. Therefore, the oxygen density is considered to be lower in the inner layer than in the outer layer.

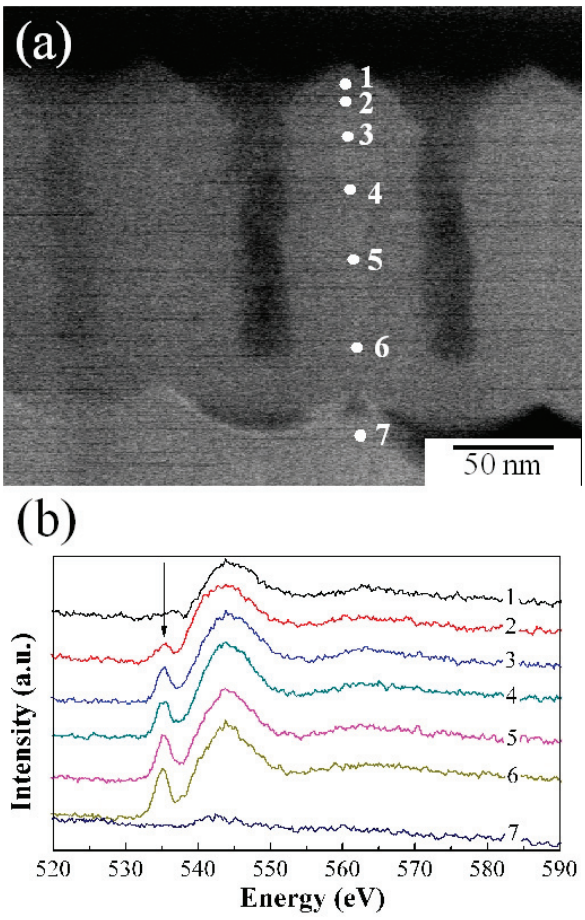

Figure 3. (a) Cross-sectional TEM image of porous alumina. (b) EELS spectra of O K-edge measured at locations 1 to 7. The arrow indicates the shoulder peaks.

3.2. Switching properties

Figure 4 shows a typical *I–V* curve for the APA memory cell at room temperature, which was obtained by changing the voltage as follows: $0 \rightarrow +9 \rightarrow 0 \rightarrow -9 \rightarrow 0$ V. We used a CRD to limit the current to 11 mA. In the positive-voltage region, the current changes from a low- (OFF) to a high- (ON) conductivity state. The current changes from the ON state to the OFF state in the negative-voltage region. This means that our samples exhibit hysteretic and bipolar behavior. Although various models were proposed to explain the resistance-switching mechanism [5,10–14], the mechanism is still unclear. Determining the conduction path in the ReRAM material is important for understanding the switching. A conducting atomic force microscopy (CAFM) measurement was carried out on the APA surface in the ON state and conduction paths were observed near triple points of the cell boundaries, which are located at the top of the inner layer [15]. The top-surface trace of the conduction paths was observed; however, their internal structure could not be probed by CAFM; other approaches are required to determine the structure. Momida *et al* modeled the electronic structure of amorphous alumina from a first-principles calculation [16]. Their simulation suggests that an unoccupied oxygen vacancy produces a subband in the band gap and plays an important

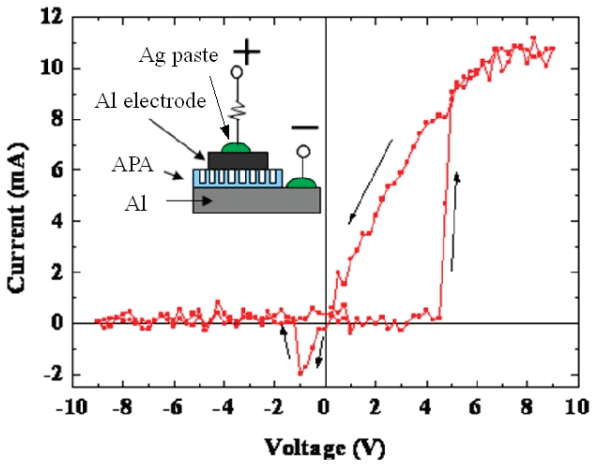

Figure 4. Typical *I–V* curve for porous alumina memory cell. The inset shows a schematic diagram of the cell.

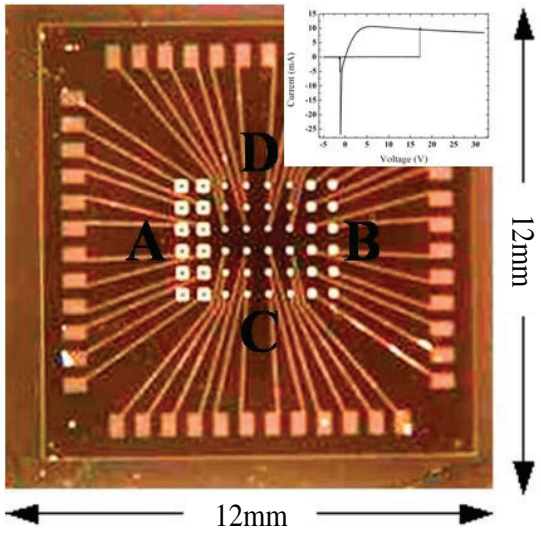

Figure 5. Optical microscope image of the pattern fabricated by photolithography (letters A, B, C and D indicate square electrodes with sides of 200, 100, 50 and 25 μm, respectively). The inset shows the *I–V* curve for the 25 μm electrode.

role in the electronic properties of amorphous alumina [17]. The existence of the subband is supported by thermally stimulated current (TSC) measurements [18]. We suggest that subbands are generated in the inner layer, where the oxygen density is lower than that in the outer layer, and that the conduction paths are produced by these subbands.

3.3. Fabrication of micropattern

For practical purposes, we have developed an APA memory cell on a SiO_2/Si substrate using conventional photolithography combined with an anodization process. The procedure is outlined as follows. (1) Anodize the Al/SiO_2/Si substrate (12 mm square) using the previously mentioned two-step process. (2) Deposit the photoresist on top of the porous alumina. (3) Bake the photoresist. (4) Expose the sample to UV light through a photomask (to form the upper contact). (5) Remove the photoresist and porous alumina layer except for the upper contact area by dry etching.

(6) Repeat steps 2 to 4. (7) Remove the photoresist. (8) Deposit the photoresist and bake. (9) Expose the sample to UV light through another photomask (to form the electrode). (10) Deposit an Al electrode by sputtering. Figure 5 shows the micrometer-scale electrode formed on the SiO_2/Si substrate. The aluminum electrodes on the patterns are squares with sides of 200, 100, 50 and 25 μm. The switching phenomenon was successfully observed for all electrode sizes, and the *I–V* curve for the 25 μm electrode is shown in the inset of figure 5. This electrode has a high set voltage and low endurance compared with those of the bulk APA memory cell. If these parameters are improved, APA ReRAM devices on Si substrates can be used in the semiconductor industry.

4. Conclusions

The nanostructure and switching characteristics of porous alumina were investigated. We fabricated a porous alumina thin film by anodization. Electron diffraction revealed that both the inner and outer layers of the film are amorphous. EELS results indicated that the inner layer contains less oxygen than the outer layer. A porous alumina memory cell exhibited hysteretic and bipolar switching. Considering previous TSC, first-principles-calculation and CAFM results, we suggest that the conduction paths of the film are located in the inner layer. We also fabricated a microscale pattern on a SiO_2/Si substrate by photolithography combined with anodization. We consider that porous alumina is a promising material for use in high-performance nonvolatile memory and other applications.

Acknowledgments

This work was performed as part of the Elements Science and Technology Project of the Ministry of Education, Culture, Sports, Science and Technology (MEXT). It was also partly supported by the 'World Premier International Research Center (WPI) Initiative on Material Nanoarchitectonics', MEXT, Japan. We thank Fukuryo Semicon Engineering Corporation for help in TEM and EELS measurements.

References

[1] Shingubara S 2003 *J. Nanopart. Res.* **5** 17
[2] Thompson G E and Wood G C 1981 *Nature* **290** 230
[3] Hickmott T W 1962 *J. Appl. Phys.* **33** 2669
[4] Kato S, Nigo S, Uno Y, Onisi T and Kido G 2006 *J. Phys.: Conf. Ser.* **38** 148
[5] Seo S *et al* 2004 *Appl. Phys. Lett.* **85** 5655
[6] Fujimoto M, Koyama H, Konagai M, Hosoi Y, Ishihara K, Ohnishi S and Awaya N 2006 *Appl. Phys. Lett.* **89** 223509
[7] Masuda H and Fukuda K 1995 *Science* **268** 1466
[8] Jollet F, Noguera C, Thromat N, Gautier M and Duraud J P 1990 *Phys. Rev.* B **42** 7587
[9] Iijima T, Kato S, Ikeda R, Ohki S, Kido G, Tansho M and Shimizu T 2005 *Chem. Lett.* **34** 1286
[10] Beck A, Bednorz J G, Gerber C, Rossel C and Widmer D 2000 *Appl. Phys. Lett.* **77** 139
[11] Liu S Q, Wu N J and Ignatiev A 2000 *Appl. Phys. Lett.* **76** 2749
[12] Baikalov A, Wang Y Q, Shen B, Lorenz B, Tsui S, Sun Y Y, Xue Y Y and Chu C W 2003 *Appl. Phys. Lett.* **83** 957
[13] Rozenberg M J, Inoue I H and Sánchez M J 2004 *Phys. Rev. Lett.* **92** 178302
[14] Fujii T, Kawasaki M, Sawa A, Akoh H, Kawazoe Y and Tokura Y 2004 *Appl. Phys. Lett.* **86** 012107
[15] Oyoshi K *J. Appl. Phys.* to be submitted
[16] Momida H, Hamada T, Takagi Y, Yamamoto T, Uda T and Ohno T 2006 *Phys. Rev.* B **73** 054108
[17] Harada Y, Nigo S, Lee J W, Kato S, Kitazawa H and Kido G *Mater. Sci. Eng.* B submitted
[18] Kato S, Nigo S, Lee J W, Mihalik M, Kitazawa H and Kido G 2008 *J. Phys.: Conf. Ser.* **109** 012017